

## Electronic Supplementary Information

### Efficient Electrochemical CO<sub>2</sub> Reduction in Acidic Electrolyte Using Armor-Like Iron Nanoparticles/Porous Nitrogen-Doped Carbon

Wenli Hao,<sup>a,b</sup> Li Peng,<sup>\*a</sup> Rongxing Qiu,<sup>a</sup> Tianwei Xue,<sup>a</sup> Ruiqing Li,<sup>a</sup> Qing-Na Zheng,<sup>a</sup> Jia Yu,<sup>c</sup>

Tongxin Qiao,<sup>a</sup> Linxiao Cui,<sup>a</sup> Yuzhong Su,<sup>a</sup> Yanzhen Hong,<sup>a</sup> Hongtao Wang,<sup>a</sup> Shuliang Yang,<sup>\*c</sup>

Jun Li<sup>\*a</sup>

<sup>a</sup> *College of Chemistry and Chemical Engineering, Xiamen University, Xiamen 361005, Fujian, PR China*

<sup>b</sup> *College of Chemistry and Chemical Engineering, Changji University, Changji 831100, China*

<sup>c</sup> *College of Energy, Xiamen University, Xiamen 361102, Fujian, PR China*

\* To whom correspondence should be addressed, Email: li.peng@xmu.edu.cn;  
ysl@xmu.edu.cn; junnyxm@xmu.edu.cn

## **Experimental section**

**Materials:** Sulfuric acid (AR), ethanol (AR), methanol (AR), dimethyl sulfoxide (AR), potassium bicarbonate (AR) and potassium chloride (AR) were purchased from Sinopharm Reagent. 2-methylimidazole (99%) was provided by Sigma-Aldrich. Ammonium nitrate (98.5%) and zinc oxide (<100nm) were obtained by Acmechem. Iron acetylacetonate (98%) and Nafion solution (5.0 wt%) were purchased from Meryer. Deuterium oxide (D<sub>2</sub>O, 99.9 atom%) was provided by Energy Chemical. Potassium thiocyanate was obtained from Aladdin. Nafion membranes (N-117) and hydrophobic conductive carbon papers (TGP-H-60) were purchased from Sinero Technology. CO<sub>2</sub> (99.999%) was provided by Fuzhou Xinhang Industrial Gases. Deionized water (18 MΩ cm<sup>-2</sup>) was used throughout this work. All chemicals used in this work were analytical grade and used without further treatments unless otherwise noted.

### **Synthesis of Fe-doped ZIF-8**

Fe-doped ZIF-8 was synthesized by mechanochemistry-assisted ball milling method. Typically, zinc oxide (40.0 mg), 2-methylimidazole (80.7 mg), and iron acetylacetonate (3.2 mg) were placed into a Teflon jar with thirty zirconia balls (5mm). The mixtures were ground for 10 min at 30 Hz using QM-2SP12 mixer mill, followed by further milling for 45 min with the addition of ethanol (45 μL) and 6.0 mg of NH<sub>4</sub>NO<sub>3</sub>. The compound was then centrifuged and washed with methanol and dried at 70 °C under vacuum for 12 h. ZIF-8 was prepared with the same synthesis procedure as for Fe-doped ZIF-8 except that iron acetylacetonate was not introduced.

### **Synthesis of Fe@NC**

Fe-doped ZIF-8 powder was transferred to a tube furnace and annealed at 1000 °C for

2 h with a heating rate of 5 °C/min under argon atmosphere. Afterward, the sample was allowed to cool naturally to room temperature, and ground in an agate mortar. The same treatment conditions were used for ZIF-8 powder sample, and the as-obtained Fe@NC and NC samples were collected and ground for further use.

### **Characterizations**

The XRD results were recorded on a Rigaku Ultima-IV powder X-ray diffractometer (XRD) with Cu K $\alpha$  radiation (0.15418 nm) with a scanning angle ( $2\theta$ ) range of 10° to 90°, a tube voltage of 40 kV, and a current of 30 mA. The samples were observed on field emission scanning electron microscope (SEM) of ZEISS Sigma of 10 kV. The morphologies of the products were observed on FEI Tecnai F30 transmission electron microscope (TEM) at an acceleration voltage of 300 kV. X-ray photoelectron spectroscopy (XPS) and Auger electron spectroscopy (AES) results for the samples were acquired on a Quantum 2000 Scanning ESCA Microprob spectrometer (Physical Electronics) with an Al K $\alpha$  X-ray radiation source ( $h\nu = 1486.6$  eV). Raman spectroscopy (Renishaw in Via instrument) results for the samples were acquired on a 785 nm excitation laser. Fe content in the samples was conducted on the inductively coupled plasma-optical emission spectrometry (ICP-OES).  $^1\text{H}$  NMR spectra results for the liquid products were operated using a Bruker AV ANCE III 500 MHz nuclear magnetic resonance spectrometer using DMSO as an internal standard. Nitrogen and CO $_2$  adsorption-desorption isotherms for the samples were measured at 77 K and 298 K using an ASAP 2020 HD88 instrument with nitrogen and helium 99.999% purity gas using the BET (Brunauer-Emmet-Teller) method to calculate the surface area. The

Fe@NC and NC electrodes for *in situ* attenuated total reflectance Fourier transform infrared spectroscopy (*in situ* ATR-FTIR) investigation in acidic electrolytes were prepared on Au film was pre-deposited onto a silicon ATR crystal by chemical deposition. The processing methods of Au film were reported by Ostwald *et al.*<sup>[S1]</sup> The *in situ* ATR-FTIR measurement was examined in a single-compartment spectroelectrochemical cell comprising three electrodes including the catalyst-deposited Si prism as working electrode, a Pt wire as the counter electrode and a standard Ag/AgCl electrode as the reference. *In situ* ATR-FTIR tests were tested in 0.2 mM H<sub>2</sub>SO<sub>4</sub> with 0.1 M KCl aqueous solution (pH = 3.4) with saturated CO<sub>2</sub>, and controlled by a CHI electrochemical workstation (CHI 660E).

### **Electrochemical measurements**

The electrochemical CO<sub>2</sub>RR measurements were carried out in CHI 660E electrochemical workstation with an H-type cell with two compartments separated by an anion exchange membrane (Nafion-117) in acidic (0.2 mM H<sub>2</sub>SO<sub>4</sub> with 0.1 M KCl (pH = 3.4)) and alkaline (0.1 M KHCO<sub>3</sub>) electrolytes. 30 mL of electrolyte was added into each compartment, respectively. Pt foil was used as counter electrodes. Ag/AgCl electrode in saturated KCl solution was used as reference electrode and carbon paper covered with catalysts was used as working electrode, respectively. In the preparation of the electrode, 10 mg of catalyst was dispersed in methanol (1920  $\mu$ L) and Nafion solution (80  $\mu$ L), followed by mixing with the assistance of ultrasonic 60 min to achieve a homogeneous solution. 100  $\mu$ L of the catalyst solution was spread evenly onto hydrophobic carbon paper (geometric area: 1 $\times$ 1 cm<sup>2</sup>) and dried at room

temperature. During the electrochemical measurements, the cathode electrolyte solution was purged with CO<sub>2</sub> for 25 min to achieve the CO<sub>2</sub> saturated solution. All measured potentials were converted to RHE using the following equation:  $E (RHE) = E (Ag/AgCl) + 0.059pH + 0.21V$ . All the gaseous phase products were routed into the gas sampling loop of a gas chromatograph and the gaseous phase composition was analyzed by GC. The separated gaseous products were analyzed by a thermal conductivity detector (for H<sub>2</sub>) and a flame ionization detector (for C<sub>2</sub>H<sub>4</sub>, CO, CH<sub>4</sub>). The Faraday efficiency of gaseous products was calculated by the equation:

$$FE = \frac{n_i \times 96485(c/mol) \times V(mL/min) \times 10^{-6}(m^3/mL) \times V(vol\%) \times 1.013 \times 10^5(N/m^2)}{8.314(N \cdot m/mol \cdot K) \times 298.15K \times j \times 60(s/min)}$$

V (vol %) = Volume concentration of CO/H<sub>2</sub> in the gas from the H-cell (GC data).

V (mL/min) = Gas flow rate measured by a flow meter at the cell at room temperature and under ambient pressure.

## Supplementary Figures and Tables

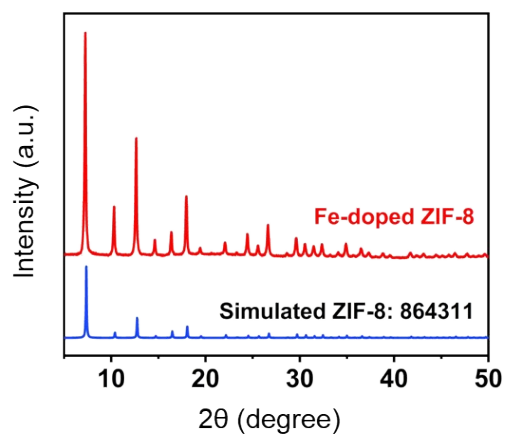


**Fig. S1** XRD patterns of simulated ZIF-8 and Fe-doped ZIF-8.

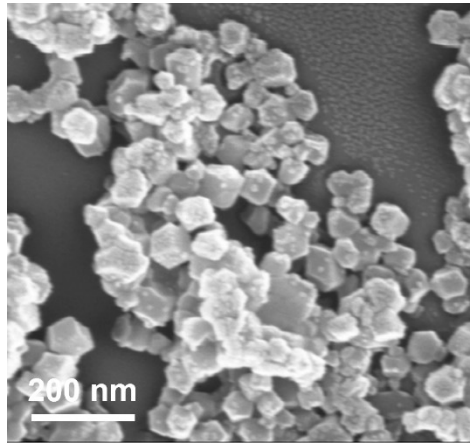


**Fig. S2** SEM image of Fe-doped ZIF-8.

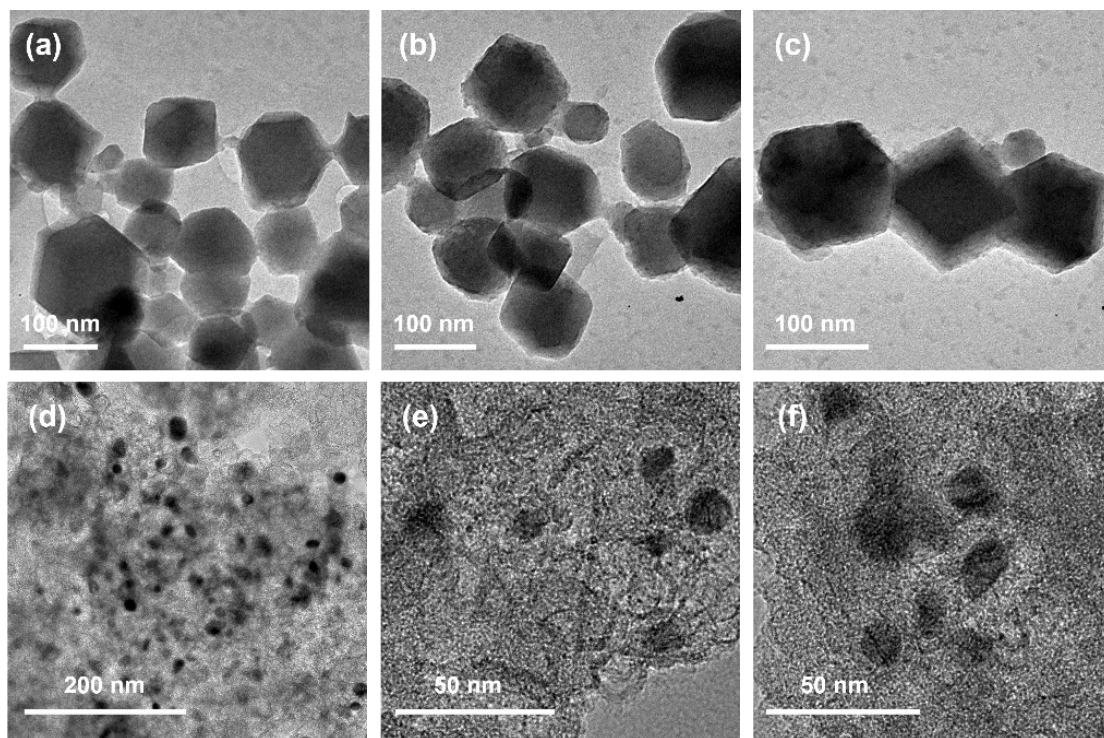


**Fig. S3** TEM images of (a-c) Fe-doped ZIF-8 and (d-e) Fe@NC in different areas.

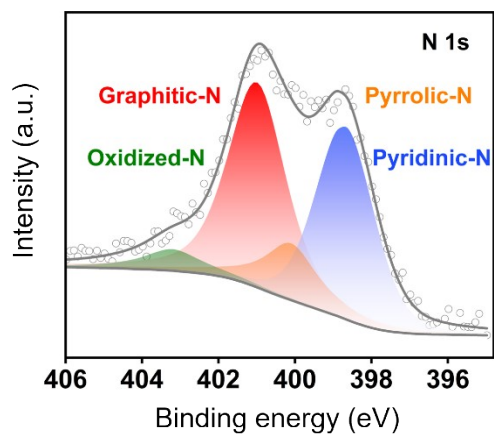


**Fig. S4** XPS spectrum of N 1s of the as-prepared NC catalyst.

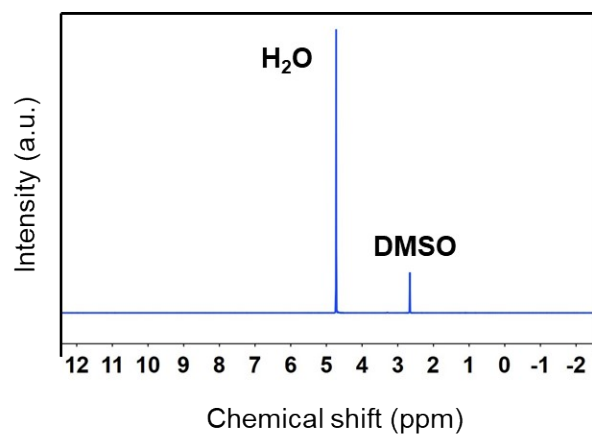


**Fig. S5** Products of Fe@NC for CO<sub>2</sub>RR were not found in the liquid phase through <sup>1</sup>H NMR with 90% water and 10% D<sub>2</sub>O as solvent and DMSO as internal standard.

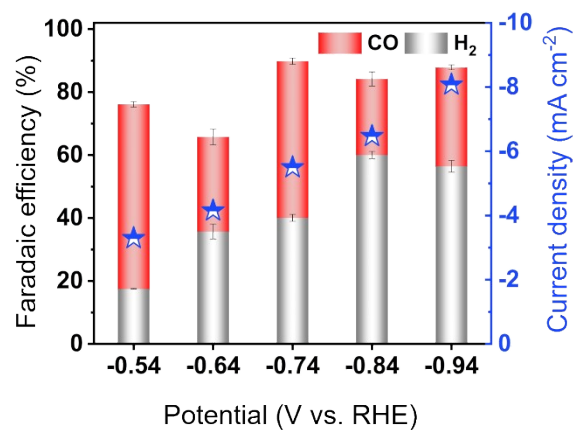


**Fig. S6** FEs at various potentials and CO current density of NC in CO<sub>2</sub>-saturated 0.1 M KHCO<sub>3</sub>.

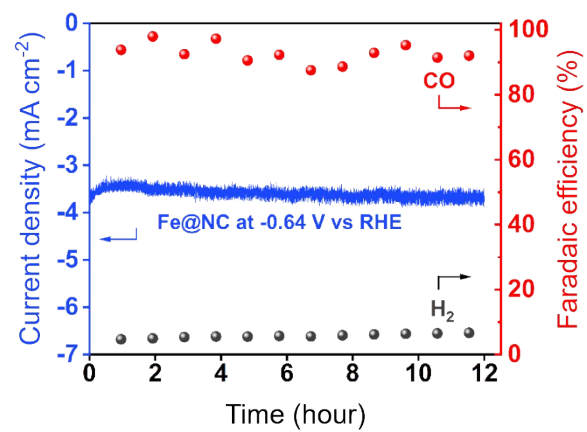


**Fig. S7** Stability test of Fe@NC performed at -0.64V vs. RHE in 0.1 M KHCO<sub>3</sub>.

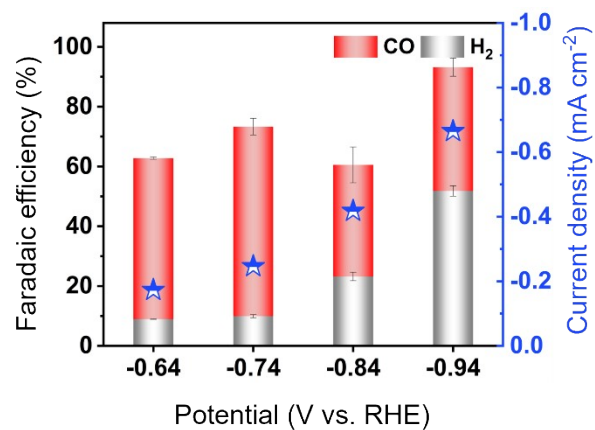


**Fig. S8** FEs at various potentials and CO current density of NC in CO<sub>2</sub>-saturated 0.2 mM H<sub>2</sub>SO<sub>4</sub> with 0.1 M KCl solutions (pH=3.4).

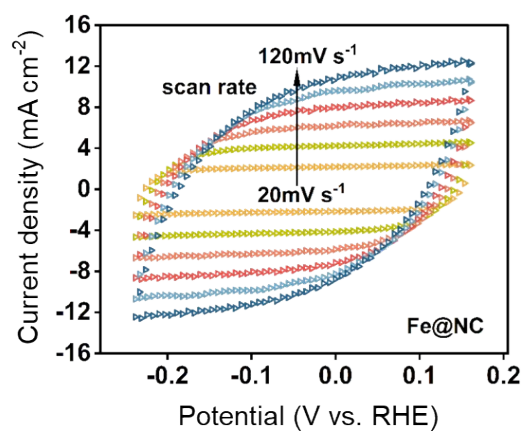


**Fig. S9** The electrochemical active specific surface area (ECSA) on the cathode measurements of Fe@NC in CO<sub>2</sub>-saturated 0.2 mM H<sub>2</sub>SO<sub>4</sub> with 0.1 M KCl solution (pH=3.4).

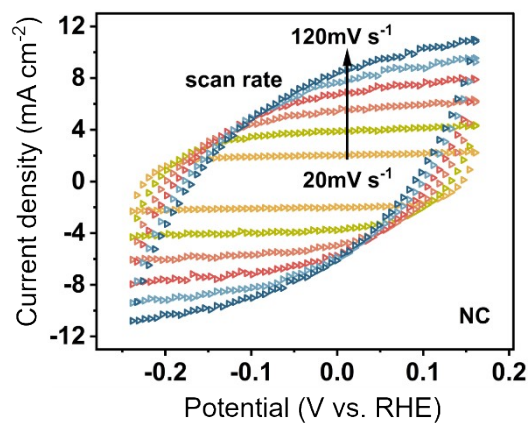


**Fig. S10** The electrochemical active specific surface area (ECSA) on the cathode measurements of NC in CO<sub>2</sub>-saturated 0.2 mM H<sub>2</sub>SO<sub>4</sub> with 0.1 M KCl solution (pH=3.4).

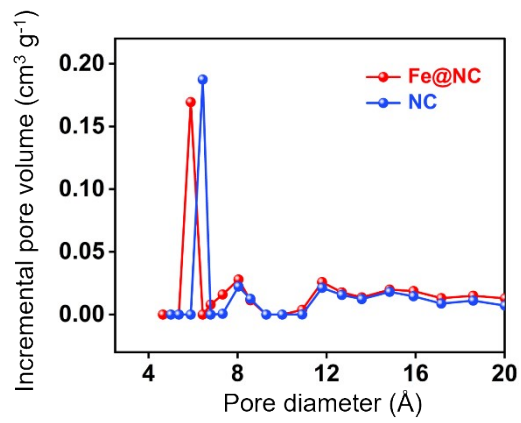


**Fig. S11** Incremental pore size distributions of Fe@NC and NC.

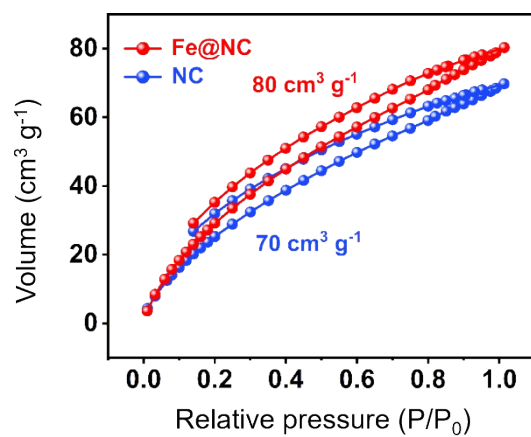


**Fig. S12** CO<sub>2</sub> adsorption and desorption isotherms measured at 298 K.

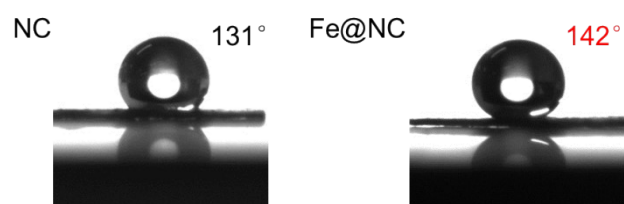


**Fig. S13** Water contact angles of NC and Fe@NC on the carbon paper.

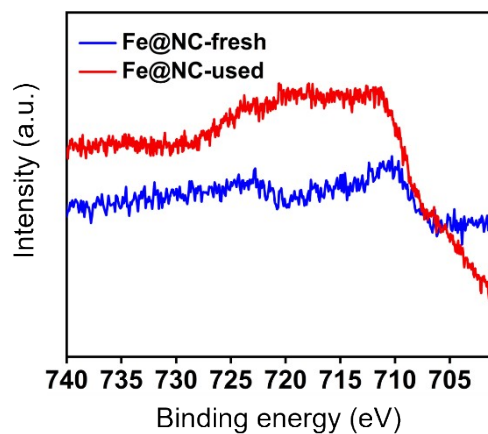


**Fig. S14** High-resolution XPS spectra of Fe 2p signal in Fe@NC-fresh (blue) and Fe@NC-used (red). The relatively weak peak intensity was due to the low loading of Fe@NC catalyst on the electrode surface.

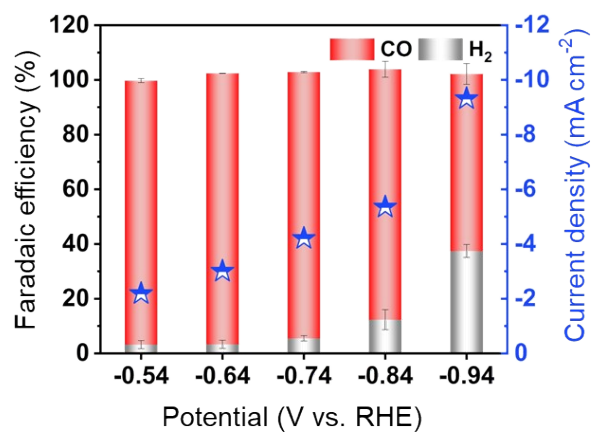


**Fig. S15** FEs at various potentials of Fe@NC and current density in 0.2 mM H<sub>2</sub>SO<sub>4</sub> with 0.1 M KCl (pH=3.4) and 0.02M KSCN at various potentials.

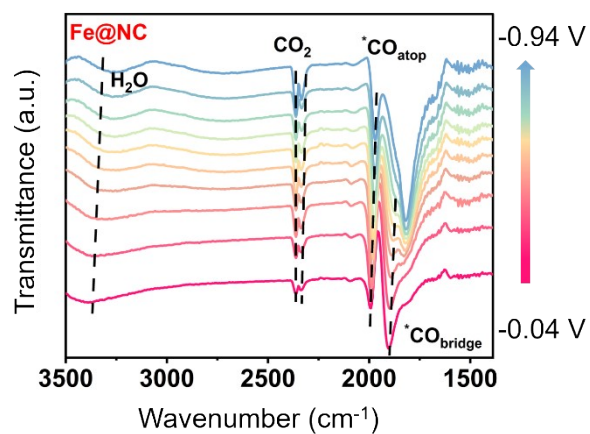


**Fig. S16** In situ FTIR spectra of Fe@NC during CO<sub>2</sub>RR at different applied potentials in acid electrolyte (0.2 mM H<sub>2</sub>SO<sub>4</sub> with 0.1 M KCl (pH=3.4)).

**Table S1** Inductively coupled plasma-optical emission spectrometry (ICP-OES)  
results on Fe@NC

Sample	Fe wt%
Fe@NC	2.47%

CO<sub>2</sub>RR Performance Evaluation**Table S2** Summary of Fe-based catalysts of CO<sub>2</sub> electroreduction

Catalysts	MOF	Main product	FE	Potential (V vs. RHE)	Ref.
<b>Fe@NC</b>	ZIF-8	CO	~99.0% in acid electrolyte ~97.0% in alkaline electrolyte	-0.64	This Work
<b>Fe<sub>2</sub>-N-C</b>	ZIF-8	CO	above 80.0%	-0.9	[S2]
<b>FeNPs-NC</b>	ZIF-8	CO	above 90.0%	-0.6	[S3]
<b>Fe<sub>1</sub>-Ni<sub>1</sub>-N-C</b>	ZIF-8	CO	96.2%	-0.5	[S4]
<b>Fe-N-C</b>	ZIF-8	CO	91.0%	-0.6	[S5]
<b>Fe-N-C</b>	/	CO	80.0%	-0.5	[S6]
<b>Fe<sub>1</sub>NC</b>	/	CO	76.0%	-0.5	[S7]
<b>Fe/NG</b>	/	CO	80.0%	-0.6	[S8]
<b>Fe-N-C</b>	ZIF-8	CO	93.5%	-0.5	[S9]
<b>Fe<sub>3</sub>C Fe<sub>1</sub>N<sub>4</sub></b>	ZIF-8	CO	94.6%	-0.5	[S10]
<b>Fe-N-C</b>	/	CO	74.0%	-0.6	[S11]

## References

- [S1] H. Miyake, S. Ye, M. Osawa. *Electrochem. Commun.*, 2002, **4**, 973-977.
- [S2] Y. Wang, B. J. Park, V. K. Paidi, R. Huang, Y. Lee, K. J. Noh, K. S. Lee, J. W. Han. *ACS Energy Lett.*, 2022, **7**, 640-649.
- [S3] Q. Fan, G. Bao, X. Chen, Y. Meng, S. Zhang, X. Ma. *ACS Catal.*, 2022, **12**, 7517-7523.
- [S4] L. Jiao, J. Zhu, Y. Zhang, W. Yang, S. Zhou, A. Li, C. Xie, X. Zheng, W. Zhou, S. H. Yu, H. L. Jiang. *J. Am. Chem. Soc.*, 2021, **143**, 19417-19424.
- [S5] T. N. Huan, N. Ranjbar, G. Rousse, M. Sougrati, A. Zitolo, V. Mougél, F. Jaouen, M. Fontecave. *ACS Catal.*, 2017, **7**, 1520-1525.
- [S6] A. S. Varela, N. Ranjbar Sahraie, J. Steinberg, W. Ju, H. S. Oh, P. Strasser. *Angew. Chem. Int. Ed.*, 2015, **54**, 10758-10762.
- [S7] S. Chen, X. Li, C. W. Kao, T. Luo, K. Chen, J. Fu, C. Ma, H. Li, M. Li, T. S. Chan, M. Liu. *Angew. Chem. Int. Ed.*, 2022, **61**, e202206233.
- [S8] C. Zhang, S. Yang, J. Wu, M. Liu, S. Yazdi, M. Ren, J. Sha, J. Zhong, K. Nie, A. S. Jalilov, Z. Li, H. Li, B. I. Yakobson, Q. Wu, E. Ringe, H. Xu, P. M. Ajayan, J. M. Tour. *Adv. Energy. Mater.*, 2018, **8**, 1703487.
- [S9] X. Qin, S. Zhu, F. Xiao, L. Zhang, M. Shao. *ACS Energy Lett.*, 2019, **4**, 1778-1783.
- [S10] J. Chen, T. Wang, X. Wang, B. Yang, X. Sang, S. Zheng, S. Yao, Z. Li, Q. Zhang, L. Lei, J. Xu, L. Dai, Y. Hou. *Adv. Funct. Mater.*, 2022, **32**, 2110174.
- [S11] J. Zhao, J. Deng, J. Han, S. Imhanria, K. Chen, W. Wang. *Chem. Eng. J.*, 2020, **389**, 124323.